

Long-period eclipsing binaries: towards the true mass-luminosity relation. II. Absolute parameters of the NN Del system

Alexei Kniazev^{1,2,3}

Abstract We present results of our study of the long-period eclipsing binary star NN Delphini (hereafter NN Del). The results are based on spectral data obtained with the HRS échelle spectrograph of the Southern African Large Telescope (SALT). Our constructed velocity curve is based on 19 spectra obtained between 2017 and 2019 years and covers all phases of the binary's orbit. The orbital period, $P = 99.252$ days, was determined from our spectral data and coincides with the period determined in previous studies, as well as the system eccentricity of $e = 0.517$. Calculated velocity amplitudes of both components allow us to determine the masses of both system components $M_1 = 1.320 M_\odot$ and $M_2 = 1.433 M_\odot$ with the accuracy about of one percent (0.8% and 1.1%), respectively. Luminosities of both components are presented as $L_1 = 4.164 L_\odot$ and $L_2 = 6.221 L_\odot$, and the effective temperatures of both components were directly evaluated ($T_{\text{eff}1} = 6545$ K and $T_{\text{eff}2} = 6190$ K) together with the metallicity of the system $[\text{Fe}/\text{H}] = -0.19$ dex and its color excess $E(B-V) = 0.026$ mag. Comparison with evolutionary tracks shows that the system age is 2.25 ± 0.19 Gyr, and both components are on the main sequence and have not yet passed the turn point. Spectral type is F5V for the hotter component and F8V for another one.

Keywords stars: luminosity function, mass function — stars: binaries: spectroscopic — stars: individual (NN Del)

1 Introduction

The ratio between the mass of a star and its luminosity on the main sequence (mass-luminosity ratio, MLR hereafter) is a fundamental law used in various fields of astrophysics. It is particularly important to restore the initial mass function (IMF) using the luminosity function (LF) of stars, and it should be noted that the IMF can only be obtained by this method, that is, through the LF and MLR.

Independent determination of the mass of a star and its luminosity is only possible for binary system components of certain types. One of these types are visual binary stars with known orbital parameters and trigonometric parallaxes (Fernandes et al. 1998; Malkov et al. 2012; Docobo et al. 2016). Usually, these stars are wide pairs, whose components do not interact with each other and, in an evolutionary sense, are similar to single stars. Another main source of independent mass determinations are detached eclipsing binary stars with components on the main sequence, whose spectra show lines of both components (double-lined eclipsing binaries, DLEB; Popper 1980; Andersen 1991; Gorda and Svechnikov 1998; Kovaleva 2001; Torres et al. 2010). These are mainly close pairs whose component's spins are synchronized by tidal interaction, and they evolve slightly different compare to single stars due to the slowdown of rotation. At the same time, for masses $M/M_\odot > 2.7$, MLR is based exclusively on the data obtained for DLEBs, and it is used for studies of single stars. Apparently, such use of MLR could be not very correct and leads to systematically wrong results when evaluating the characteristics of stars in the discussed mass range, as well as when restoring the initial mass function with its help. For example, Malkov (2003) compared the radii of DLEBs and single stars and found a noticeable difference between the observation parameters of the B0V-G0V components of the DLEBs and single stars of similar spectral classes.

Alexei Kniazev

¹South African Astronomical Observatory, PO Box 9, 7935 Observatory, Cape Town, South Africa.

²Southern African Large Telescope Foundation, PO Box 9, 7935 Observatory, Cape Town, South Africa.

³Sternberg Astronomical Institute, Lomonosov Moscow State University, Moscow, Russia.

Table 1 Parameters of NN Del system collected from the literature.

Parameter	GF (2003) ^a	G(2014) ^b	S(2018) ^c	G(2019) ^d
Orbital period P (d)	99.2684±0.0005	99.244±0.019	99.26849±0.00015	99.2690±0.0009
Eccentricity e	0.51759±0.00002	0.5168±0.0029	0.51944±0.00055	0.5197±0.0004
Rad. vel. semi-amplitude K_1 (km s ⁻¹)	–	39.45±0.27	39.62±0.15	39.407±0.037
Rad. vel. semi-amplitude K_2 (km s ⁻¹)	–	36.04±0.21	36.22±0.11	36.191±0.023
Systemic heliocentric vel. γ (km s ⁻¹)	–	–8.19±0.08	–9.405±0.050	–9.485±0.015
Inclination i (degrees)	89.488±0.003	90.0 (fixed)	89.6342±0.0076	89.90±0.11
The longitude of the periastron ω (degrees)	171.710±0.005	170.0±0.4	169.75±0.45	170.00±0.07
R.m.s. residuals of Keplerian fit (km s ⁻¹)	–	0.56	0.11	0.10 (0.18)
m_1 (M _⊙) (Component A)	–	1.328±0.021	1.337±0.011	1.3266±0.0021
m_2 (M _⊙) (Component B)	–	1.454±0.025	1.462±0.013	1.4445±0.0029
r_1	0.01584±0.00006	–	0.01260±0.00015	–
r_2	0.0153	–	0.01720±0.00015	–
T_{eff} (K) (Component A)	6437±5	–	–	–
T_{eff} (K) (Component B)	6500.0	–	–	–
log g (dex) (Component A)	–	–	4.1532±0.0051	–
log g (dex) (Component B)	–	–	3.9226±0.0035	–
Radius R (R _⊙) (Component A)	2.2	–	1.604±0.014	–
Radius R (R _⊙) (Component B)	2.2	–	2.188±0.015	–
$v \sin i$ (km s ⁻¹) (Component A)	–	7.7±0.6	–	–
$v \sin i$ (km s ⁻¹) (Component B)	–	7.4±0.3	–	–
Spectral Type	F5 IV (both)	F8 IV-V (both)	–	–

^a – Gómez-Forrellad et al. (2003); ^b – Griffin (2014); ^c – Sybilski et al. (2018); ^d – Gallenne et al. (2019)

Malkov (2007) collected data on fundamental parameters of 19 components of long-period DLEB. These stars presumably have not undergone synchronization of rotation with the orbital period and therefore rotate rapidly and evolve similarly to single stars. Possibly, only such kind of data should be used to construct relations (in particular, MLR) for “isolated” stars for masses $M/M_{\odot} > 2.7$. The masses of the components of other types of binary stars (orbital, resolved spectral binaries) rarely exceed this limit. Note that of the 19 DLEB stars mentioned above, only 13 have a mass greater than 2.7 M/M_{\odot} , which is clearly insufficient to draw any definite conclusions. For this reason, we have begun a systematic study of long-period DLEB stars to obtain their mass and luminosity parameters and to compare these parameters with those obtained for short-period DLEB stars. The definition of the test sample as well as a brief description of the software package FBS created to analyze spectra of binary stars is described in our first paper (Kniazhev et al. 2020). Here, we present the first results obtained for the long-period eclipsing binary star NN Del, which belongs to our test sample and has some previously published studies to help evaluate the accuracy of the parameters based on our spectral data. Hereafter we call the brighter star in the DLEB system NN Del component A.

2 Previous studies of NN Del

The system NN Del (HD 197952, HIP 102545) was discovered as variable based on HIPPARCOS satellite data (Makarov et al. 1994), but the only information published was the star changing its brightness by more than half of a magnitude. The brightness curve for the NN Del system was obtained and thoroughly studied by Gómez-Forrellad et al. (2003). They concluded that both components of the system are almost equal to each other, the period of the system is 99.268 days and the eccentricity of the system is 0.5176, i.e. the stellar components have non-circular orbits. Gómez-Forrellad et al. (2003) also determined the types of each star as F5, based on photometric data, and since the radii of both components were calculated to be 2.2 R_{\odot} , which meant that both stars had already left the main sequence, their luminosity class was defined as IV. Table 1 shows all parameters and errors, for NN Del that were defined by Gómez-Forrellad et al. (2003) and following works, where this binary system was studied.

Griffin (2014) carried out spectroscopy of NN Del using a photoelectric spectrometer designed to measure the radial velocities of stars (Griffin 1967). It should be noted here that the spectra were not obtained, but the velocities of both components were determined. In total, 37 measurements were made during three years, and for the first time a velocity curve was constructed and masses of both components were determined. The

Table 2 HRS observations for NN Del and found heliocentric velocities

Date	MJD	Exp.time	V_{hel1}	V_{hel2}
(1)	(2)	(3)	(4)	(5)
20170504	2457878.65465	315.	43.528 ± 0.012	-68.014 ± 0.025
20170508	2457882.63785	315.	38.422 ± 0.012	-61.257 ± 0.026
20170520	2457894.64881	400.	-2.161 ± 0.045	-16.526 ± 0.041
20170805	2457971.46249	315.	12.869 ± 0.013	-34.007 ± 0.034
20170814	2457980.36746	450.	42.930 ± 0.016	-66.858 ± 0.029
20170830	2457996.37722	315.	-7.087 ± 0.023	-12.431 ± 0.039
20170927	2458024.28117	315.	-25.935 ± 0.017	8.459 ± 0.021
20171003	2458030.27510	315.	-26.714 ± 0.017	9.568 ± 0.024
20171024	2458051.23722	240.	-23.874 ± 0.019	5.794 ± 0.035
20180428	2458237.66367	315.	-28.411 ± 0.029	8.636 ± 0.056
20180429	2458238.65980	315.	-27.308 ± 0.014	8.903 ± 0.031
20180926	2458388.33887	315.	3.222 ± 0.014	-23.580 ± 0.024
20180930	2458392.23932	315.	-5.554 ± 0.016	-15.491 ± 0.031
20181007	2458399.29359	315.	-14.738 ± 0.016	-5.158 ± 0.032
20181015	2458407.27283	315.	-21.292 ± 0.015	2.574 ± 0.027
20190728	2458693.50237	315.	-10.364 ± 0.041	-8.896 ± 0.070
20190801	2458697.46381	315.	-14.558 ± 0.016	-4.101 ± 0.031
20190810	2458706.45261	315.	-21.766 ± 0.016	3.275 ± 0.030
20190818	2458714.44764	315.	-24.539 ± 0.014	7.221 ± 0.030

final accuracy of the velocity curve (scattering of residuals after model subtraction) was 0.56 km sec^{-1} . The obtained values of the orbital period P and eccentricity e agreed with numbers found from photometric data (Gómez-Forrellad et al. 2003), where the inclination i of the system was assumed to be 90 degrees, but the longitude ω of the periastron w was different at the 4σ level, although Griffin (2014) noted the unbelievable high accuracy of all the parameters given by Gómez-Forrellad et al. (2003).

Sybilski et al. (2018) carried out spectral observations of NN Del using the échelle spectrograph CHIRON ($R \sim 80000$) installed on the 1.5m telescope of CTIO observatory (Chile). Only seven observations were taken, but the spectroscopy was combined with photometry from Gómez-Forrellad et al. (2003) to construct both the velocity and the brightness curves simultaneously. The obtained masses of both components of the system agreed with those obtained by Griffin (2014) taking into account errors. The accuracy of the velocity curve was 0.11 km sec^{-1} that is much higher compare to Griffin (2014). The use of spectral and photometric data together made it possible to determine masses of both components and their radii, although the authors noted that defining all these characteristics was not the main purpose of their work. For the same reason, the authors did not try to estimate temperatures and luminosities of both

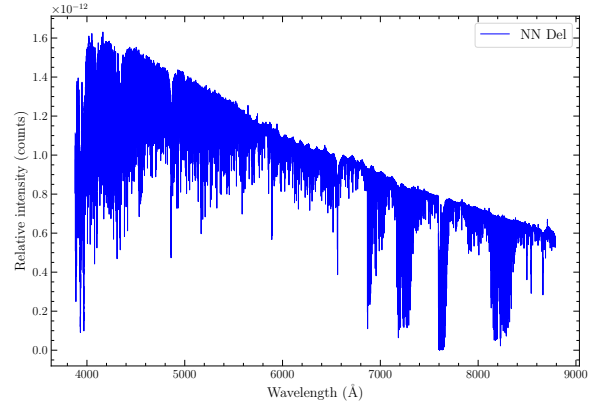


Fig. 1 An example of a fully processed spectrum of NN Del. The spectrum consists of 70 échelle orders from both blue and red arms merged together and corrected for sensitivity.

components from the obtained spectra, and presented only the ratio of the luminosities of the components as $L_B/L_A = 1.6564 \pm 0.0076$.

Gallenne et al. (2019) is the most recent work in which the characteristics of the NN Del system were defined. In that paper spectral data were obtained with the échelle spectrograph STELLA ($R \sim 55000$) and were used along with interferometric data obtained with VLTI/PIONIER. 40 échelle spectra were taken during

2014–2018. The simultaneous use of spectral and astrometric data allowed the determination of the masses of both components and the distance to NN Del. The accuracy of the velocity curve was 0.10 km sec^{-1} for component A and 0.18 km sec^{-1} for component B, which made it possible to determine the masses of the components with an accuracy of 0.18%, and the distance to the system NN Del with an accuracy of 0.4%. It was noted that the resulting parallax is greater than the parallax in *Gaia* DR2 (Gaia Collaboration 2018), but agrees with the estimate obtained by HIPPARCOS. Further, Gallenne et al. (2019) tried to evaluate the evolutionary status of both components of NN Del. They used their own mass estimates of both components, obtained with high accuracy and adopted temperatures, fractional radii and luminosities for both components of NN Del. Finally, after analysis of all available data, it was concluded that both components of the NN Del system are on the main sequence and have not yet passed the turn point.

3 Spectral observations and data reduction

Spectral observations of NN Del were made during 2017–2019 at the Southern African Large Telescope (SALT; Buckley et al. 2006; O’Donoghue et al. 2006) using the fiber échelle spectrograph HRS (Barnes et al. 2008; Bramall et al. 2010, 2012; Crause et al. 2014). HRS is a thermostabilised dual-beam échelle spectrograph. The blue arm of the spectrograph covers the spectral range 3900–5550 Å, and the red arm covers the spectral range 5550–8900 Å, respectively. HRS is equipped with four pairs of fibers (object fiber and sky fiber) and can be used in low (LR), medium (MR), high resolution (HR) and high stability modes. All spectral observations of NN Del were taken with MR mode ($R=36\,500\text{--}39\,000$), with fibers with a diameter of 2.23 arcseconds. Both the blue arm and the red arm CCDs were used with binning 1×1 . The dates of observations, their Julian days, and exposure times are presented in Table 2.

Since HRS is the vacuum échelle spectrograph that is installed inside a temperature-controlled enclosure, all standard calibrations are performed once a week, which is enough to achieve an accuracy 300 m/sec for MR mode. The primary HRS data reduction was done automatically using the standard SALT pipeline described by Crawford et al. (2010). The following échelle data reduction was performed using the standard HRS data pipeline described in detail by Kniazev et al. (2016, 2019).

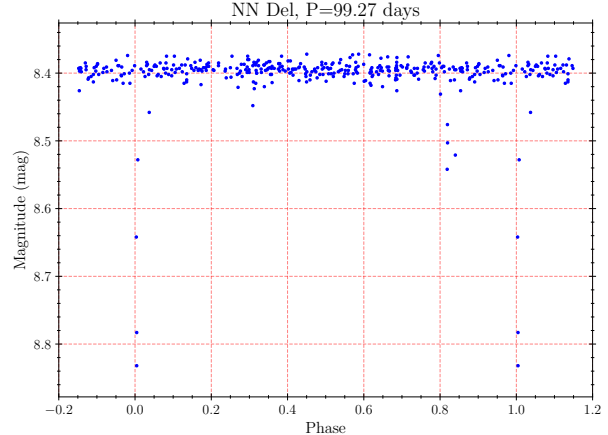


Fig. 2 Photometric data from the ASAS survey converted to the period $P=99.27$ days. There are only few points that can indicate the shape of the primary and secondary minima.

Each HRS spectrum of NN Del was additionally corrected for bad columns and pixels and was also corrected for the spectral sensitivity curve obtained closest to the date of the observation. Spectrophotometric standards for HRS are observed once a week as part of the HRS Calibration Plan. An example of a fully processed spectrum of NN Del, which was used in further analysis, is shown in Figure 1. The spectrum consists of 70 échelle orders from both the blue and the red arm merged together and corrected for sensitivity. Unfortunately, SALT is a telescope where the unfilled entrance pupil of the telescope moves during the observation. For that reason, absolute flux calibration is not feasible with SALT. However, since all optical elements are always the same, relative flux calibration can be used for SALT data. Additionally, since HRS is a fiber-fed échelle spectrograph, the relative distribution of energy could be done with high enough accuracy (Kniazev 2020; in preparation).

4 Available photometric data

Unfortunately, there are no good photometric data for NN Del among all existing public surveys. The best available data are from the ASAS survey (Pojmanski 1997) as shown in Figure 2. It is obvious, that even these data have too few points outlining the positions and shapes of the narrow primary and secondary minima and it is impossible to use these data for any modeling. Therefore, it was decided to use our spectral data together with the results of the analysis of photometric data from Gómez-Forrellad et al. (2003), which were also used by Sybilski et al. (2018).

5 Spectral data analysis

To investigate the fully processed HRS spectra we used FBS (Fitting Binary Stars) software specially developed by our group (Katkov et al. 2020 in preparation) and partially described in Kniazev et al. (2020). This program uses a library of theoretically calculated high-resolution stellar spectra and is designed to determine radial velocities and stellar parameters (T_{eff} , $\log g$, $v \sin i$, $[\text{Fe}/\text{H}]$) for both components of the binary system, and parameters $E(\text{B}-\text{V})$ and $W_{1,2}$ that describe the reddening of both spectra and the contribution of each component to the observed spectrum at the wavelength of 5500 Å that is very close to the effective wavelength for the V-filter. By definition, $W_1 + W_2 = 1$. The program simultaneously approximates the observed spectrum by a model, which is obtained by interpolating over the grid of stellar models and convolves it with a function that takes into account broadening caused by the rotation of a star ($v \sin i$) with a shift corresponding to a specific value of the radial velocity at a given epoch. In case of a binary star, the fitting routine uses two model spectra for the components, each with its own radial velocity and stellar atmosphere parameters, and as result the observed spectrum is decomposed into separate spectra of two components. If there are several spectra of the binary system obtained at different epochs, the program finds a solution, in which the parameters (T_{eff} , $\log g$, $v \sin i$, $[\text{Fe}/\text{H}]$, W)_{1,2} and $E(\text{B}-\text{V})$ satisfy all spectra that can be fitted simultaneously, and velocities of both components $V_{1,2}^j$ are determined for each particular epoch j . The present study uses theoretical stellar models from Coelho (2014).

6 Results of our study of NN Del

The measured heliocentric velocities for both components of the system NN Del and their errors are presented for each epoch in Table 2. To determine the velocities, as well as the parameters of the components and orbital parameters of the binary system NN Del, we used the iterative procedure described below. The necessity of this iterative procedure was due to two facts: (1) We used only spectral observations, but to obtain the complete set of parameters to calculate masses and luminosity, a simultaneous analysis of spectral and photometric data is necessary, as was done, for example, by Sybilski et al. (2018). Potentially, masses for both components can be obtained by analyzing simultaneously spectral and astrometric data, as was done by Gallenne et al. (2019), but for the further analysis of the evolutionary status of NN Del these authors were still forced

to use the parameters derived by Sybilski et al. (2018). (2) The presence of known temperature- $\log g$ degeneration for stars colder than about 7000 K. With the full set of spectral and photometric data in hands, this degeneration can be avoided.

Our iterative procedure was as follows:

1. During the first iteration, the program FBS was used only with one limitation – it was assumed that both components had the same metallicity ($[\text{Fe}/\text{H}]_1 \equiv [\text{Fe}/\text{H}]_2$; (Hawkins et al. 2020)). All 19 obtained spectra were fitted simultaneously and 19 velocities were obtained for both components together with the parameters of both components (T_{eff} , $\log g$, $v \sin i$, $[\text{Fe}/\text{H}]$)_{1,2}. The result of the analysis of a single spectrum is shown as an example in Figure 3. The upper panel of the figure shows the result of the fit in the spectral range 4000-5300 Å, and the bottom panel shows the result of the same fit in the H β line region. In each panel, the black and red lines correspond to the observed spectrum and its model. The blue and orange lines refer to the model spectra of the first and second component, respectively. The bottom part of each panel shows the difference between observed spectrum and its model with a black line, where blue lines indicate errors in the observed spectrum.
2. Based on the obtained velocities and their errors, the radial velocity curves for both components were constructed using the program FBS, and the orbital parameters of the system and their errors were calculated. Parameters such as the orbital period P , velocity semi-amplitudes of both components K_1 and K_2 , system eccentricity e , system heliocentric velocity γ and the longitude of the periastron ω were obtained.
3. Using previously determined P , e , K_1 and K_2 and the inclination angle i (taken from research by Sybilski et al. 2018), the masses of M_1 and M_2 of both components and their errors were determined by the equations:

$$\begin{aligned} M_1 &= 1.036149 \cdot 10^{-7} (K_1 + K_2)^2 K_2 P e^{3/2} \sin^{-3}(i) \\ M_2 &= 1.036149 \cdot 10^{-7} (K_1 + K_2)^2 K_1 P e^{3/2} \sin^{-3}(i) \end{aligned} \quad (1)$$

Here $M_{1,2}$ is in M_{\odot} , $K_{1,2}$ is in km/s, P is in day.

4. Next the absolute sizes of the major and minor axes of the NN Del system were calculated as:

$$\begin{aligned} a_1 &= 0.01976569 K_1 P e^{1/2} \sin^{-1}(i) \\ a_2 &= 0.01976569 K_2 P e^{1/2} \sin^{-1}(i) \end{aligned} \quad (2)$$

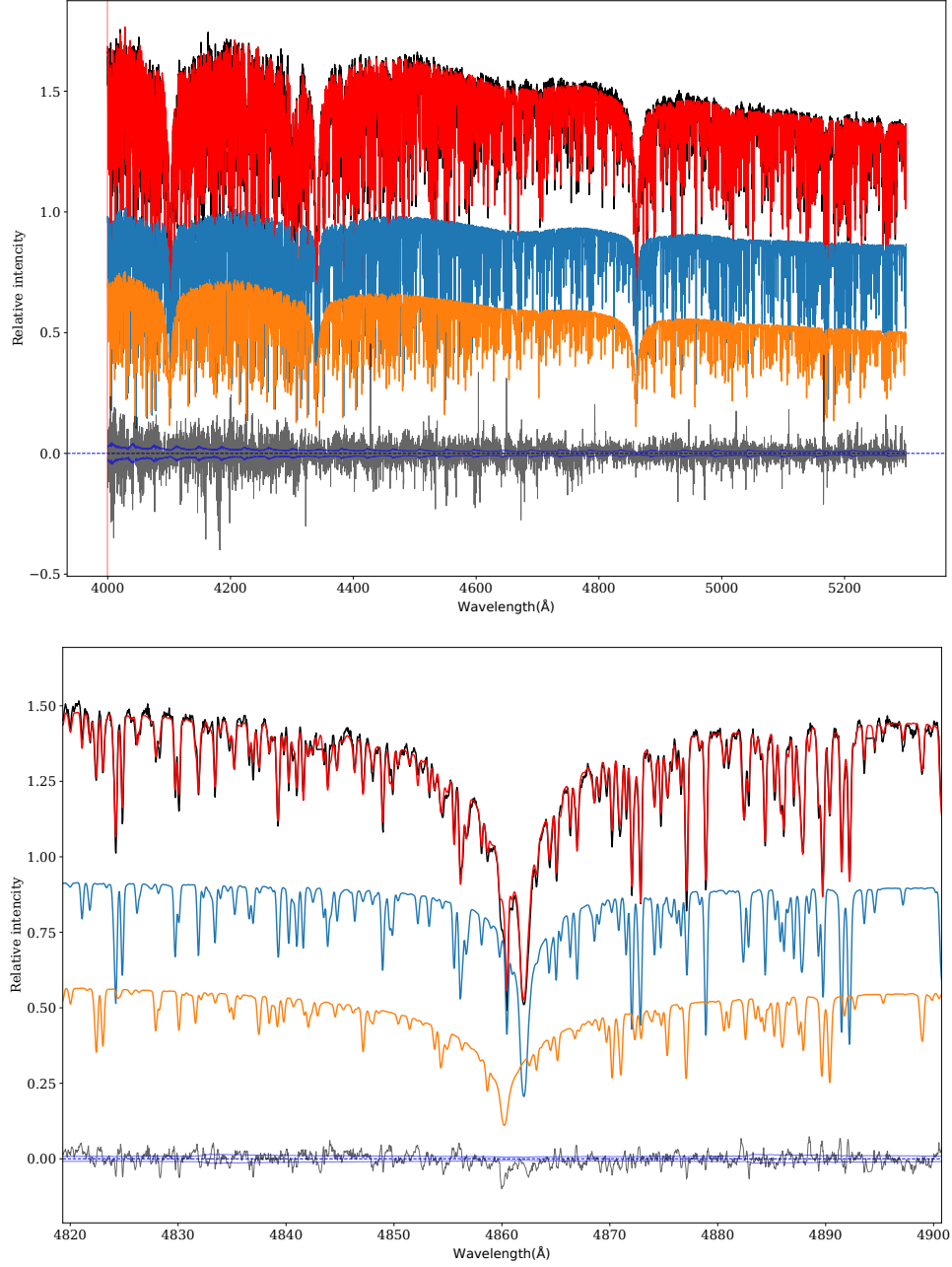


Fig. 3 The results of the analysis of one spectrum of NN Del obtained with HRS. The upper panel shows the result of the fit in the spectral region 4000-5300 Å, and the bottom panel shows a small spectral region near the H β line. In each panel, the black and red lines correspond to the observed spectrum and its model, respectively. The orange and blue lines refer to the model spectra of the first and second component, respectively. The bottom part of each panel shows the difference between observed spectrum and its model with a black line, where blue lines indicate errors in the observed spectrum.

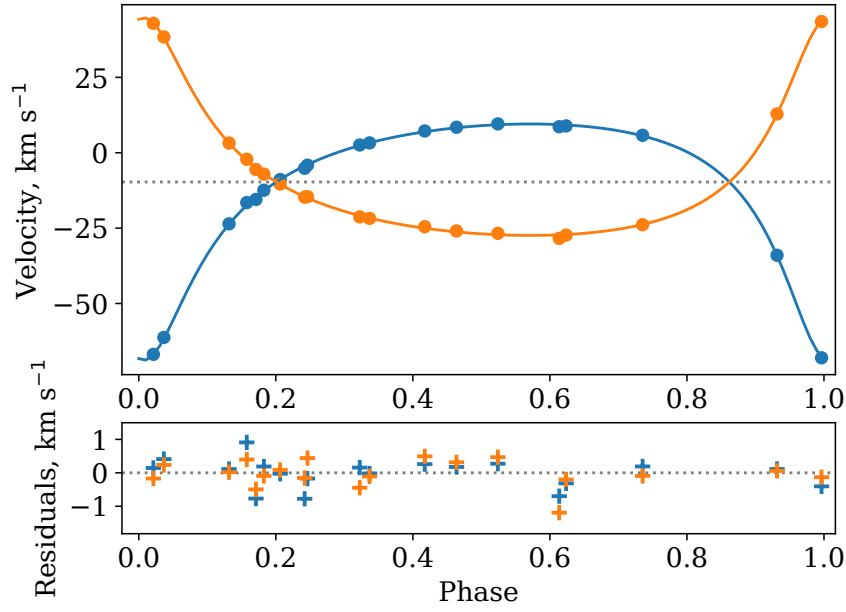


Fig. 4 The final radial velocity curve for NN Del as the function of phase. The fitted parameters are shown in Table 4. The model is constructed by the points listed in Table 2. The velocity curve of component A is shown in orange, and the velocity curve of component B is shown in blue. The differences between the model and the observed points are shown in the bottom panel. The final accuracy of the velocity curve (residuals after model subtraction) is 0.494 km s^{-1} , what is close to the nominal accuracy of 0.300 km s^{-1} for HRS spectra obtained in MR mode (Kniazev et al. 2019).

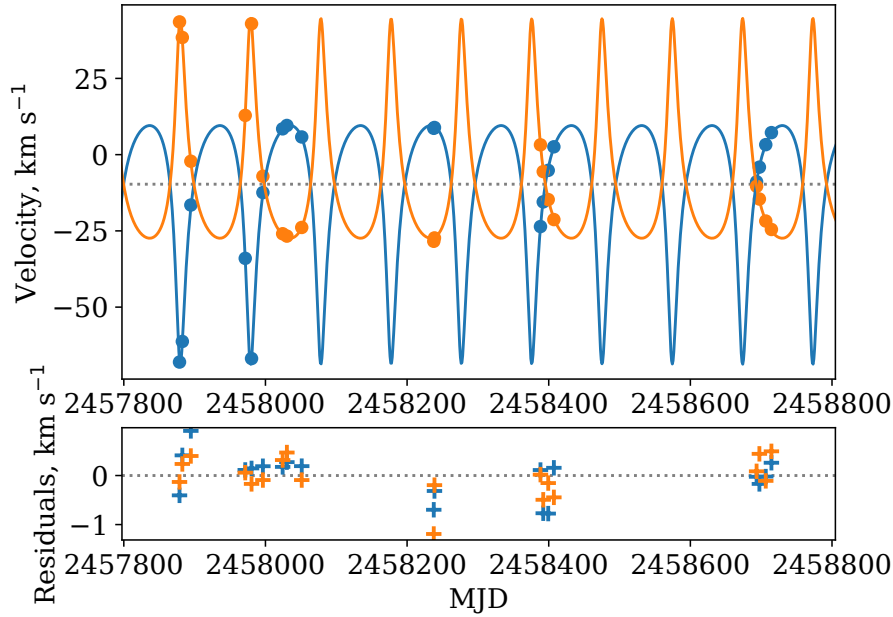


Fig. 5 The final radial velocity curve for NN Del as the function of Julian date. Designations are the same as in Figure 4. From this figure one can see that the observations were made during ten periods of NN Del.

as well as the radii R_1 and R_2 for both components:

$$\begin{aligned} R_1 &= r_1 * (a_1 + a_2) \\ R_2 &= r_2 * (a_1 + a_2) \end{aligned} \quad (3)$$

where the relative radii (r_1/r_2) for both components were taken from Sybilski et al. (2018), since they used both photometric and spectral data simultaneously, and their relative radii are more correct compare to the ones from Gómez-Forrellad et al. (2003). Here $a_{1,2}$ and $R_{1,2}$ is in R_\odot .

5. Finally, $\log g_1$ and $\log g_2$ were recalculated using:

$$\begin{aligned} \log g_1 &= 4.438068 + \log M_1 - 2 \log R_1 \\ \log g_2 &= 4.438068 + \log M_2 - 2 \log R_2 \end{aligned} \quad (4)$$

Numerical coefficients of Eqs. (1,2,4) are taken from Prša et al. (2016) and based on the IAU 2015 Resolution B3 on Recommended Nominal Conversion Constants for Selected Solar and Planetary Properties (Mamajek et al. 2015).

If the new values were different from the previous values by more than 0.01 dex, all step were repeated, with the new, fixed, values for $\log g_1$ and $\log g_2$. When the difference between the old and new $\log g_1$ and $\log g_2$ was less of 0.01 dex, the procedure was stopped and all calculated parameters were declared as the final ones. The final heliocentric velocities for both components are presented in Table 2 with their errors.

Since the output errors of the FBS program are fitting errors, which are often underestimated, errors of the output parameters need to be estimated in more realistic way. A statistical evaluation was used, where all possible pairs of the observed spectra were taken, parameters $\log g_{1,2}$ were fixed and these pairs were fitted by the program. With 19 observed spectra 171 different pairs were fitted. After that, for each solution, the parameter q (mass ratio of the components) was calculated as:

$$q = -(V_1 - \gamma)/(V_2 - \gamma), \quad (5)$$

Table 3 Parameters for both stellar components.

Parameter	Component A	Component B
T_{eff} (K)	6545 ± 180	6190 ± 85
$\log T_{\text{eff}}$ (K)	3.82 ± 0.02	3.79 ± 0.01
$\log g$ (dex)	4.16 ± 0.01	3.92 ± 0.01
$v \sin i$ (km s $^{-1}$)	1.15 ± 0.13	0.36 ± 0.28
W (at 5550 Å)	0.378 ± 0.009	0.622 ± 0.009
[Fe/H] (dex)	-0.19 ± 0.05	
E(B-V)	0.026 ± 0.002	

where γ is the systemic heliocentric velocity of the NN Del system.

Unstable solutions far from $q = 1$ were discarded (approximately 30% of decisions) iteratively with a clipping level of 2.5σ , and all other solutions were used to calculate the average and its error for each of the parameters (T_{eff} , $v \sin i$, [Fe/H] $_{1,2}$ and E(B-V). The final calculated errors are given in Table 3. The calculated radial velocity curves as a function of phase and Julian date are shown in Figures 4 and 5, respectively. The final accuracy of the velocity curve (scatter of the points after model subtraction) was $0.406 \text{ km sec}^{-1}$, which is close to the nominal accuracy of 0.300 km s^{-1} for HRS spectra obtained in MR mode (Kniazhev et al. 2019). The values for the orbital parameters of the binary star NN Del and their errors are given in Table 4.

With all the values of the physical parameters of the NN Del system and their errors, as well as the orbital parameters of the system, the masses and radii of both components were calculated by Eq.1–3. Using the obtained radii and temperatures, the luminosity of each of the components was then calculated as:

$$L(\text{spec}) = R^2 \left(\frac{T_{\text{eff}}}{5780} \right)^4, \quad (6)$$

where T_{eff} of the Sun is 5780 K. The obtained absolute parameters of the NN Del system are presented in Table 5.

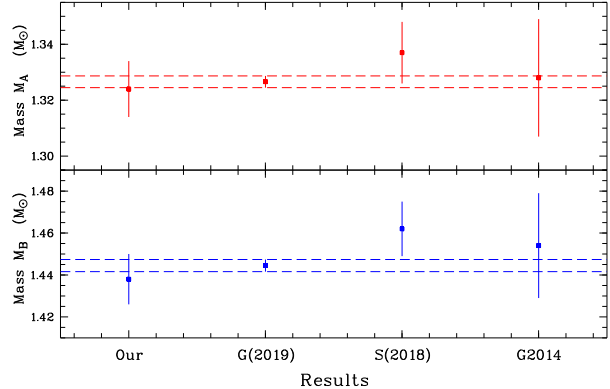


Fig. 6 Comparison of our mass measurement for both components of NN Del with previously published results (see Table 1 for more details).

7 Discussion

7.1 Comparison of parameters for the NN Del system

To evaluate the correctness of our orbital parameters calculation program, we fitted the 40 radial velocities

Table 4 Best-fit orbital elements.

Parameter	Value	%
Epoch at radial velocity maximum T_0 (d)	2457779.76 ± 0.06	0.00
Orbital period P (d)	99.252 ± 0.024	0.02
Eccentricity e	0.517 ± 0.002	0.38
Radial velocity semi-amplitude $K1$ (km s $^{-1}$)	39.191 ± 0.179	0.46
Radial velocity semi-amplitude $K2$ (km s $^{-1}$)	36.101 ± 0.099	0.27
Systemic heliocentric velocity γ (km s $^{-1}$)	-9.692 ± 0.066	0.68
The longitude of the periastron ω (degrees)	170.307 ± 0.532	0.31
Root-mean-square residuals of Keplerian fit (km s $^{-1}$)	0.406	–

of the system NN Del given in Table A.2 of Gallenne et al. (2019) and obtained full agreement with the orbital elements presented in Gallenne et al. (2019) up to the final accuracy of the velocity curves: 0.10 km sec $^{-1}$ for the component A and 0.18 km sec $^{-1}$ for the component B.

It was obvious from the beginning, that since we use échelle spectra with over twice lower resolution compare of the CHIRON échelle spectrograph ($R \sim 80000$) used by Sybilski et al. (2018) and about one and a half times lower than the resolution of the STELLA échelle spectrograph ($R \sim 55000$) used by Gallenne et al. (2019), our accuracy of the obtained parameters could be worse or comparable to the accuracy obtained by those authors. Figure 6 shows a comparison of our mass estimates for both components of NN Del with previously published results. It can be seen that our mass estimates do not show any systematics and are in very good agreement with the most accurate values obtained by Gallenne et al. (2019), with differences not exceeding 1σ of the total error. That also means that the radial velocity semi-amplitudes determined by us do not show any systematics and positively characterize the quality of HRS data.

With found absolute parameters of the system NN Del, we can try to check their correctness. First, using the distance to NN Del according to *Gaia* DR2 (the parallax 5.6393 ± 0.0636 is translated to a distance 177.33 ± 2.00 parsec; Gaia Collaboration 2018) as well as the color excess $E(B - V)$ resulting from our study, we can estimate the absolute magnitude of NN Del as $M(V) = 2.08 \pm 0.03$ mag. Since we know from our spectral data the contributions (parameter W in Table 3) of each component at the equivalent wavelength of the V-band, we can separate the resulting absolute magnitude into contributions of each component. Taking into account the bolometric corrections from (Straižys 1992) for the T_{eff} , presented in Table 3, we are then able to calculate their luminosities (photometric luminosities hereafter; $L_{1,2}(\text{phot})$) and compare these luminosities with the spectral luminosities ($L_{1,2}(\text{spec})$) obtained by Eq.6. We obtain $L_2(\text{phot}) = 7.05 \pm 0.20 L_{\odot}$

and $L_2(\text{phot}) = 4.28 \pm 0.15 L_{\odot}$, which agree with the luminosities $L_{1,2}(\text{spec})$ presented in Table 5. From these photometric luminosities it is possible to calculate photometric radii using Eq.6 and temperatures of the components from Table 3 as $R_2(\text{phot}) = 2.31 \pm 0.07 R_{\odot}$ and $R_1(\text{phot}) = 1.61 \pm 0.07 R_{\odot}$. As can be seen from the comparison of luminosities and radii, given in Table 5, both spectral and photometric luminosities and radii of the component A agree with a difference of only 0.3σ and 0.5σ . The spectral and photometric luminosities and radii of the component B are slightly less agreeable at about 2.0σ and 2.2σ , respectively, but are still close to each other. Such a comparison of absolute parameters, counted in a different way and matched to each other, is a good indicator of the correctness of the absolute parameters found for the NN Del system.

We can also independently estimate the distance to NN Del and compare it with the distance from *Gaia* DR2 (Gaia Collaboration 2018). Our estimation of the distance could be done with use of the known total V_{tot} magnitude, found extinction shown in Table 3 and an absolute magnitude $M(V_{\text{tot}})$. The $M(V_{\text{tot}})$ could be found as the sum of absolute magnitudes for both components $M(V_{1,2})$, where the absolute magnitude for each component could be calculated with use of luminosities based on the spectroscopic radii $L_{\text{(spec)}}$ from Table 5 and temperatures T_{eff} from Table 3 and bolometric corrections calculated with use of (Straižys 1992). The final result is also shown in Table 5. Our estimated distance is smaller than the distance according to *Gaia* and this result is in the agreement with the result obtained by Gallenne et al. (2019) as $d = 167.99 \pm 0.65$ pc. However, we have to admit here that the large error of our assessment means that difference we found is not significant with a difference of only 1.62σ .

In the Torres et al. (2010) review the data on luminosities and masses of 190 stars, from 95 DLEB systems, have been collected. A comparison of our obtained characteristics for NN Del with data from Torres et al. (2010), as presented in Figure 7, shows that our

Table 5 The absolute parameters for NN Del

Parameter	Value	%
$M_1 (M_\odot)$	1.320 ± 0.011	0.83
$M_2 (M_\odot)$	1.433 ± 0.015	1.06
$\log M_1$	0.121 ± 0.004	—
$\log M_2$	0.156 ± 0.005	—
$a_1 (R_\odot)$	65.813 ± 0.315	0.48
$a_2 (R_\odot)$	60.624 ± 0.188	0.31
$R_1(\text{spec}) (R_\odot)$	1.594 ± 0.016	1.00
$R_2(\text{spec}) (R_\odot)$	2.176 ± 0.018	0.82
$\log R_1(\text{spec})$	0.203 ± 0.004	—
$\log R_2(\text{spec})$	0.338 ± 0.004	—
$R_1(\text{phot}) (R_\odot)$	1.614 ± 0.070	4.35
$R_2(\text{phot}) (R_\odot)$	2.314 ± 0.071	3.06
$\log R_1(\text{phot})$	0.208 ± 0.019	—
$\log R_2(\text{phot})$	0.364 ± 0.013	—
$L_1(\text{spec}) (L_\odot)$	4.164 ± 0.346	8.31
$L_2(\text{spec}) (L_\odot)$	6.221 ± 0.371	5.96
$\log L_1(\text{spec})$	0.620 ± 0.036	—
$\log L_2(\text{spec})$	0.794 ± 0.026	—
$L_1(\text{phot}) (L_\odot)$	4.280 ± 0.151	3.53
$L_2(\text{phot}) (L_\odot)$	7.051 ± 0.205	2.90
$\log L_1(\text{phot})$	0.631 ± 0.015	—
$\log L_2(\text{phot})$	0.848 ± 0.013	—
Distance (pc)	169.71 ± 4.27	2.52
Age (Gyr)	2.25 ± 0.19	8.44
Spectral Type (A)	F5	—
Spectral Type (B)	F8	—

characteristics of the NN Del components are fully consistent with the masses, luminosities and radii of the stars in this large sample.

7.2 Evolutionary state

Since NN Del is a detached system where components do not influence each other's evolution, it is reasonable to assume that evolutionary status of each component can be assessed based on evolutionary models of single stars. Since Gallenne et al. (2019) showed that results from the models PARSEC (PADova and TRIeste Stellar Evolution Code, Bressan et al. 2012), BaSTI (Bag of Stellar Tracks and Isochrones, Pietrinferni et al. 2004) and MIST (MESA Isochrones and Stellar Tracks, Choi et al. 2016) agree well, we only used the MIST model in our work. Since the masses of the NN Del components are known to us with the highest degree of accuracy, we retrieved from MIST¹ the evolutionary tracks for stars of these masses and considered the positions of each of

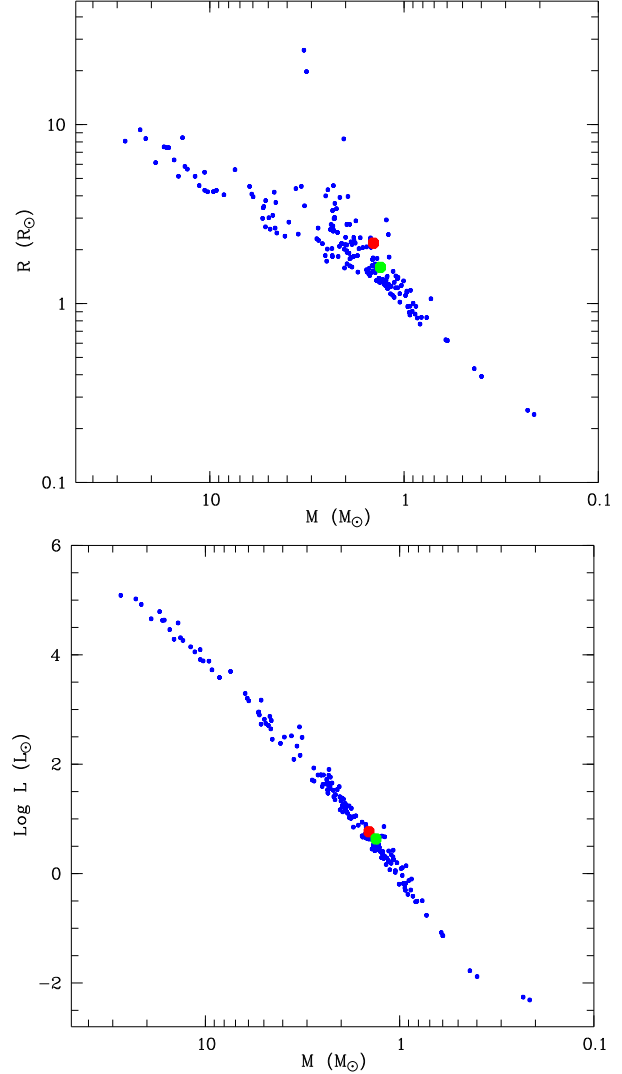


Fig. 7 Diagram for all stars from Torres et al. (2010) with position of both components of NN Del. Component A shown in green and component B in red. Sizes of the symbols are significantly larger than the errors.

the components on these tracks, varying the metallicity $[\text{Fe}/\text{H}]$ from -0.2 to 0.2 dex in increments of 0.05 dex. We then searched for the minimum of the equation:

$$\chi^2 = \sum_{i=1}^2 \left[\left(\frac{\Delta L}{\sigma_L} \right)_i^2 + \left(\frac{\Delta T_{\text{eff}}}{\sigma_{T_{\text{eff}}}} \right)_i^2 + \left(\frac{\Delta R}{\sigma_R} \right)_i^2 + \left(\frac{\Delta g}{\sigma_g} \right)_i^2 \right], \quad (7)$$

where the summation is done on both components ($i = 1, 2$), the symbol Δ shows the logarithmic difference between the model and the value obtained from the observations, and σ is also used in the logarithmic scale. The search was performed for each model metallicity under the assumption that both components of the system have the same metallicity.

¹http://waps.cfa.harvard.edu/MIST/interp_isos.html

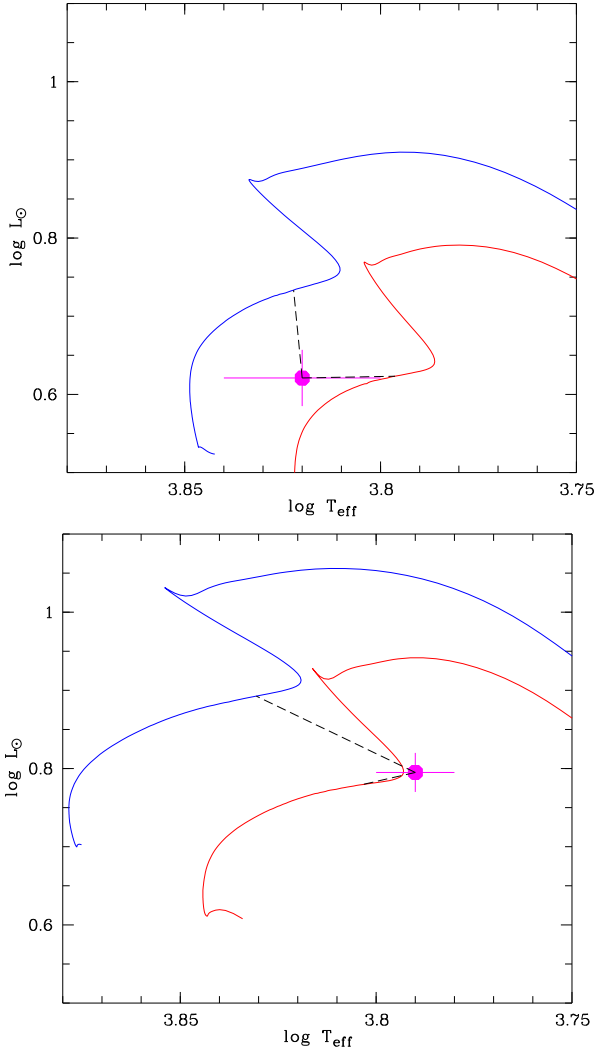


Fig. 8 Evolutionary tracks of stars of mass $1.44 M_{\odot}$ (upper panel) for the component A and mass $1.32 M_{\odot}$ (lower panel) for the component B for two metallicities: $[Fe/H] = -0.19$ dex (blue) and $[Fe/H] = 0.05$ dex (red). The burgundy dots include the NN Del system components, and the black dotted lines show the distance to the optimal solution as found by Eq. 7.

Figure 8 shows the $\log L$ – $\log T_{\text{eff}}$ plot for two solutions: (1) for metallicity $[Fe/H] = -0.19$ dex, which is derived from our star models (see Section 6) and (2) for metallicity $[Fe/H] = 0.05$ dex, which showed the best χ^2 from Eq. 7. For metallicity $[Fe/H] = -0.19$ dex, the age of the system NN Del is estimated to be 2.06 Gyr, and for $[Fe/H] = 0.05$ dex it is 2.44 Gyr. In both cases, as can be seen in Figure 8, both components have not yet passed the turn point and are on the main sequence, which coincides with the conclusion by Gallenne et al. (2019).

It is possible to explain the resulting difference in metallicities by the systematic shift between the metallicity scales of the stellar models from Coelho (2014) and the MIST models. We therefore took stellar models from PHOENIX Husser et al. (2013) and recalculated our data according to the methodology described in Sections 5 and 6, and resulted the value $[Fe/H] = -0.20$ dex as well. We would like to note that the PHOENIX models match the observed spectra less well and therefore we prefer to work with the models from Coelho (2014). As the final result, we adopt the age assessment for the NN Del system as $t_{\text{avg}} = 2.25 \pm 0.19$ Gyr, which also agrees with the output from Gallenne et al. (2019).

Since FBS software splits observational spectrum into two separate components (see Figure 3) and we know that both of them have luminosity class V, we can estimate the spectral type of each of them. For both components $\text{Ca K}/(\text{H}\epsilon + \text{Ca H})$ intensity ratio ~ 1 , but the CH G-band at $\sim 4300 \text{ \AA}$ is not clear visible yet implies that both spectra have spectral types F0–F5 (Evans and Howarth 2003; Evans et al. 2004). Additionally, taking into account criteria from Jaschek and Jaschek (1990) about EWs of different lines, I finally classify the component A as F5 based on $\text{EW}(\text{Fe I } \lambda 4045) = 0.51 \pm 0.02 \text{ \AA}$, $\text{EW}(\text{Sr II } \lambda 4077) = 0.31 \pm 0.02 \text{ \AA}$, $\text{EW}(\text{H}\gamma) = 4.95 \pm 0.10 \text{ \AA}$ and $\text{EW}(\text{H}\beta) = 5.15 \pm 0.10 \text{ \AA}$ and component B as F8 based on $\text{EW}(\text{Fe I } \lambda 4045) = 0.71 \pm 0.01 \text{ \AA}$, $\text{EW}(\text{Ca I } \lambda 4226) = 0.75 \pm 0.02 \text{ \AA}$, $\text{EW}(\text{H}\gamma) = 4.20 \pm 0.10 \text{ \AA}$ and $\text{EW}(\text{H}\beta) = 4.05 \pm 0.10 \text{ \AA}$. This classification for component A coincides with the classification from Gómez-Forrellad et al. (2003) and for components B with the classification from Griffin (2014).

8 Conclusions

The long-period eclipsing binary star NN Del has been studied using spectral data obtained with the HRS échelle spectrograph of the SALT telescope. A velocity curve has been constructed which is based on 19 spectra obtained during 2017–2019 years and covers all phases of this binary system. The obtained orbital and

absolute parameters of the components, together with their errors, agree with the results obtained in early works, which shows the good quality of HRS spectra and correctness of the applied processing and analysis methodology. The luminosities of both components are calculated and the effective temperatures are directly evaluated altogether with the metallicity of the system. The analysis of the calculated parameters is presented that allows to estimate the obtained absolute parameters in various ways and shows the repeatability of these assessments. The age and evolutionary status of both components have been estimated, as well as their spectral types.

Acknowledgments

A.K. is grateful to D.Graczyk (the referee) for useful comments and suggestions on the manuscript. This work is based on observations obtained with the Southern African Large Telescope (SALT) under programs 2017-1-MLT-001 and 2019-1-SCI-004 (PI: Kniazev). This research is supported by the National Research Foundation (NRF) of South Africa and the Russian Foundation for Basic Research grant 19-02-00779.

References

- Andersen, J.: *Astron. Astrophys. Rev.* **3**, 91 (1991). doi:10.1007/BF00873538
- Barnes, S.I., Cottrell, P.L., Albrow, M.D., Frost, N., Graham, G., Kershaw, G., Ritchie, R., Jones, D., Sharples, R., Bramall, D., Schmoll, J., Luke, P., Clark, P., Tyas, L., Buckley, D.A.H., Brink, J.: The optical design of the Southern African Large Telescope high resolution spectrograph: SALT HRS. *Society of Photo-Optical Instrumentation Engineers (SPIE) Conference Series*, vol. 7014, p. 70140 (2008). doi:10.1117/12.788219
- Bramall, D.G., Sharples, R., Tyas, L., Schmoll, J., Clark, P., Luke, P., Looker, N., Dipper, N.A., Ryan, S., Buckley, D.A.H., Brink, J., Barnes, S.I.: The SALT HRS spectrograph: final design, instrument capabilities, and operational modes. *Society of Photo-Optical Instrumentation Engineers (SPIE) Conference Series*, vol. 7735, p. 77354 (2010). doi:10.1117/12.856382
- Bramall, D.G., Schmoll, J., Tyas, L.M.G., Clark, P., Younger, E., Sharples, R.M., Dipper, N.A., Ryan, S.G., Buckley, D.A.H., Brink, J.: The SALT HRS spectrograph: instrument integration and laboratory test results. *Society of Photo-Optical Instrumentation Engineers (SPIE) Conference Series*, vol. 8446, p. 84460 (2012). doi:10.1117/12.925935
- Bressan, A., Marigo, P., Girardi, L., Salasnich, B., Dal Cero, C., Rubele, S., Nanni, A.: *Mon. Not. R. Astron. Soc.* **427**(1), 127 (2012). 1208.4498. doi:10.1111/j.1365-2966.2012.21948.x
- Buckley, D.A.H., Swart, G.P., Meiring, J.G.: Completion and commissioning of the Southern African Large Telescope. *Society of Photo-Optical Instrumentation Engineers (SPIE) Conference Series*, vol. 6267, p. 62670 (2006). doi:10.1117/12.673750
- Choi, J., Dotter, A., Conroy, C., Cantiello, M., Paxton, B., Johnson, B.D.: *Astrophys. J.* **823**(2), 102 (2016). 1604.08592. doi:10.3847/0004-637X/823/2/102
- Coelho, P.R.T.: *Mon. Not. R. Astron. Soc.* **440**(2), 1027 (2014). 1404.3243. doi:10.1093/mnras/stu365
- Crause, L.A., Sharples, R.M., Bramall, D.G., Schmoll, J., Clark, P., Younger, E.J., Tyas, L.M.G., Ryan, S.G., Brink, J.D., Strydom, O.J., Buckley, D.A.H., Wilkinson, M., Crawford, S.M., Depagne, É.: Performance of the Southern African Large Telescope (SALT) High Resolution Spectrograph (HRS). *Society of Photo-Optical Instrumentation Engineers (SPIE) Conference Series*, vol. 9147, p. 91476 (2014). doi:10.1117/12.2055635
- Crawford, S.M., Still, M., Schellart, P., Balona, L., Buckley, D.A.H., Dugmore, G., Gulbis, A.A.S., Kniazev, A., Kotze, M., Loaring, N., Nordsieck, K.H., Pickering, T.E., Potter, S., Romero Colmenero, E., Vaisanen, P., Williams, T., Zietsman, E.: PySALT: the SALT science pipeline. *Society of Photo-Optical Instrumentation Engineers (SPIE) Conference Series*, vol. 7737, p. 773725 (2010). doi:10.1117/12.857000
- Docobo, J.A., Tamazian, V.S., Malkov, O.Y., Campo, P.P., Chulkov, D.A.: *Mon. Not. R. Astron. Soc.* **459**, 1580 (2016). 1609.03392. doi:10.1093/mnras/stw709
- Evans, C.J., Howarth, I.D.: *Mon. Not. R. Astron. Soc.* **345**(4), 1223 (2003). astro-ph/0308125. doi:10.1046/j.1365-2966.2003.07038.x
- Evans, C.J., Howarth, I.D., Irwin, M.J., Burnley, A.W., Harries, T.J.: *Mon. Not. R. Astron. Soc.* **353**(2), 601 (2004). astro-ph/0406409. doi:10.1111/j.1365-2966.2004.08096.x
- Fernandes, J., Lebreton, Y., Baglin, A., Morel, P.: *Astron. Astrophys.* **338**, 455 (1998)
- Gaia Collaboration: *Astron. Astrophys.* **616**, 11 (2018). 1804.09380. doi:10.1051/0004-6361/201832865
- Gallenne, A., Pietrzyński, G., Graczyk, D., Pilecki, B., Storm, J., Nardetto, N., Taormina, M., Gieren, W., Tkachenko, A., Kervella, P., Mérand, A., Weber, M.: *Astron. Astrophys.* **632**, 31 (2019). 1910.03393. doi:10.1051/0004-6361/201935837
- Gómez-Forrellad, J.M., Sánchez-Bajo, F., Corbera-Subirana, M., García-Melendo, E., Vidal-Sainz, J.: *Astrophys. Space Sci.* **283**(2), 297 (2003). doi:10.1023/A:1021324730755
- Gorda, S.Y., Svechnikov, M.A.: *Astronomy Reports* **42**, 793 (1998)
- Griffin, R.F.: *Astrophys. J.* **148**, 465 (1967). doi:10.1086/149168
- Griffin, R.F.: *The Observatory* **134**, 109 (2014)
- Hawkins, K., Lucey, M., Ting, Y.-S., Ji, A., Katzberg, D., Thompson, M., El-Badry, K., Teske, J., Nelson, T., Carrillo, A.: *Mon. Not. R. Astron. Soc.* **492**(1), 1164 (2020). 1912.08895. doi:10.1093/mnras/stz3132
- Husser, T.-O., Wende-von Berg, S., Dreizler, S., Homeier, D., Reiners, A., Barman, T., Hauschildt, P.H.: *Astron. Astrophys.* **553**, 6 (2013). 1303.5632. doi:10.1051/0004-6361/201219058
- Jaschek, C., Jaschek, M.: *The Classification of Stars*, (1990)
- Kniazev, A.Y., Gvaramadze, V.V., Berdnikov, L.N.: *Mon. Not. R. Astron. Soc.* **459**(3), 3068 (2016). 1604.03942. doi:10.1093/mnras/stw889
- Kniazev, A.Y., Usenko, I.A., Kovtyukh, V.V., Berdnikov, L.N.: *Astrophysical Bulletin* **74**(2), 208 (2019). doi:10.1134/S199034131902010X
- Kniazev, A.Y., Malkov, O.Y., Katkov, I.Y., Berdnikov, L.N.: arXiv e-prints, 2004 (2020). 2004.04115
- Kovaleva, D.A.: *Astronomy Reports* **45**, 972 (2001). doi:10.1134/1.1426128
- Makarov, V., Bastian, U., Hoeg, E., Grossmann, V., Wicenc, A.: *Information Bulletin on Variable Stars* **4118**, 1 (1994)
- Malkov, O.Y.: *Astron. Astrophys.* **402**, 1055 (2003). doi:10.1051/0004-6361:20030313
- Malkov, O.Y.: *Mon. Not. R. Astron. Soc.* **382**, 1073 (2007). doi:10.1111/j.1365-2966.2007.12086.x
- Malkov, O.Y., Tamazian, V.S., Docobo, J.A., Chulkov, D.A.: *Astron. Astrophys.* **546**, 69 (2012). doi:10.1051/0004-6361/201219774
- Mamajek, E.E., Prsa, A., Torres, G., Harmanec, P., Asplund, M., Bennett, P.D., Capitaine, N., Christensen-Dalsgaard, J., Depagne, E., Folkner, W.M., Haberster, M., Hekker, S., Hilton, J.L., Kostov, V., Kurtz, D.W., Laskar, J., Mason, B.D., Milone, E.F., Montgomery, M.M., Richards, M.T., Schou, J., Stewart, S.G.: arXiv e-prints, 1510 (2015). 1510.07674

-
- O'Donoghue, D., Buckley, D.A.H., Balona, L.A., Bester, D., Botha, L., Brink, J., Carter, D.B., Charles, P.A., Christians, A., Ebrahim, F., Emmerich, R., Esterhuyse, W., Evans, G.P., Fourie, C., Fourie, P., Gajjar, H., Gordon, M., Gumede, C., de Kock, M., Koeslag, A., Koorts, W.P., Kriel, H., Marang, F., Meiring, J.G., Menzies, J.W., Menzies, P., Metcalfe, D., Meyer, B., Nel, L., O'Connor, J., Osman, F., Du Plessis, C., Rall, H., Riddick, A., Romero-Colmenero, E., Potter, S.B., Sass, C., Schalekamp, H., Sessions, N., Siyengo, S., Sopela, V., Steyn, H., Stoffels, J., Scholtz, J., Swart, G., Swat, A., Swiegers, J., Tiheli, T., Vaisanen, P., Whittaker, W., van Wyk, F.: *Mon. Not. R. Astron. Soc.* **372**(1), 151 (2006). [astro-ph/0607266](#). doi:10.1111/j.1365-2966.2006.10834.x
- Pietrinferni, A., Cassisi, S., Salaris, M., Castelli, F.: *Astrophys. J.* **612**(1), 168 (2004). [astro-ph/0405193](#). doi:10.1086/422498
- Pojmanski, G.: *Acta Astron.* **47**, 467 (1997). [astro-ph/9712146](#)
- Popper, D.M.: *Annu. Rev. Astron. Astrophys.* **18**, 115 (1980). doi:10.1146/annurev.aa.18.090180.000555
- Prša, A., Conroy, K.E., Horvat, M., Pablo, H., Kochoska, A., Bloemen, S., Giammarco, J., Hambleton, K.M., Degroote, P.: *Astrophys. J. Suppl. Ser.* **227**(2), 29 (2016). 1609.08135. doi:10.3847/1538-4365/227/2/29
- Straizys, V.: *Multicolor Stellar Photometry*, (1992)
- Sybilski, P., Pawłaszek, R.K., Sybilska, A., Konacki, M., Helminiak, K.G., Kozłowski, S.K., Ratajczak, M.: *Mon. Not. R. Astron. Soc.* **478**(2), 1942 (2018). 1805.00520. doi:10.1093/mnras/sty1135
- Torres, G., Andersen, J., Giménez, A.: *Astron. Astrophys. Rev.* **18**, 67 (2010). 0908.2624. doi:10.1007/s00159-009-0025-1